JCB Article

Identification of amino acid residues lining the pore of a gap junction channel

I.M. Skerrett,[1] J. Aronowitz,[1] J.H. Shin,[1] G. Cymes,[2] E. Kasperek,[1] F.L. Cao,[3] and B.J. Nicholson[1]

[1]Department of Biological Sciences, State University of New York at Buffalo, Buffalo, NY 14260
[2]Department of Physiology and Biophysics, State University of New York at Buffalo, Buffalo, NY 14214
[3]Department of Genetics, Emory School of Medicine, Atlanta, GA 30322

Gap junctions represent a ubiquitous and integral part of multicellular organisms, providing the only conduit for direct exchange of nutrients, messengers and ions between neighboring cells. However, at the molecular level we have limited knowledge of their endogenous permeants and selectivity features. By probing the accessibility of systematically substituted cysteine residues to thiol blockers (a technique called SCAM), we have identified the pore-lining residues of a gap junction channel composed of Cx32. Analysis of 45 sites in perfused *Xenopus* oocyte pairs defined M3 as the major pore-lining helix, with M2 (open state) or M1 (closed state) also contributing to the wider cytoplasmic opening of the channel. Additional mapping of a close association between M3 and M4 allowed the helices of the low resolution map (Unger et al., 1999. *Science*. 283:1176–1180) to be tentatively assigned to the connexin transmembrane domains. Contrary to previous conceptions of the gap junction channel, the residues lining the pore are largely hydrophobic. This indicates that the selective permeabilities of this unique channel class may result from novel mechanisms, including complex van der Waals interactions of permeants with the pore wall, rather than mechanisms involving fixed charges or chelation chemistry as reported for other ion channels.

Introduction

Gap junctions are arrays of intercellular channels that have been identified in every metazoan phylum. As such, they are likely to be required for many aspects of intercellular communication necessary for multicellular life. Graphic illustrations of this have been provided in both vertebrates (mice) and invertebrates (*Caenorhabditis elegans* and *Drosophila melanogaster*) using genetic ablation of the genes encoding their components (connexins, or Cx [Eiberger et al., 2001], and innexins [Phelan and Starrich, 2001], respectively). These "knockouts" have induced a variety of defects in the heart, lens, liver, placenta, body musculature, and nervous system (for reviews see Spray et al., 2000; Phelan and Starrich, 2001). In humans, the association of Cx26/Cx30/Cx31 mutations with autosomal deafness in some cases and epidermal disease in others, connexin 32 (Cx32)* mutations with a congenital demyelinating neuropathy, and Cx50 mutations with congenital cataracts confirms their widespread significance (Kelsell et al., 2001).

Unlike other channels, gap junctions do not have well defined permeability properties, as they allow the passage of ions and metabolites as large as 1,000 D between cells. Yet it has become apparent that they are not nonspecific. In fact, selectivity may be manifested as modest (up to 10-fold) charge selectivity (Veenstra, 1996; Suchyna et al., 1999), different size restrictions for permeants (from ~300 to >1,000 D; Steinberg et al., 1994; Elfgang et al., 1995; Bevans et al., 1998; Nicholson et al., 2000), and even dramatic selectivity (up to 100-fold) for natural metabolites (Bevans et al., 1998; Goldberg et al., 1999). These differences in selectivity are consistent with the observation that different connexins cannot always functionally substitute for one another (e.g., heart function [Plum et al., 2000]; lens cataracts [White, 2002]).

Defining the molecular basis of selectivity is critical to understanding the role of gap junctions. This requires the identification of the pore-lining residues with which permeants interact. The membrane topology of the connexin subunits (four transmembrane spans with cytoplasmic NH_2 and COOH termini) and basic structure of the gap junction channel (two hexameric hemichannels dock in the extracellular

Address correspondence to B.J. Nicholson, Dept. of Biological Sciences, 615 Cooke Hall, State University of New York at Buffalo, Buffalo, NY 14260-1300. Tel.: (716) 645-3344. Fax: (716) 645-2871. E-mail: bjn@acsu.buffalo.edu

*Abbreviations used in this paper: Cx32, connexin32; Gj, junctional conductance; MBB, maleimidobutyryl biocytin; SCAM, substituted cysteine accessibility method; Vj, transjunctional voltage.

Key words: connexin32; SCAM; pore lining; accessibility; *Xenopus* oocyte expression

gap to form the intercellular pore) are well established (Yeager and Nicholson, 1996; Sosinsky, 2000). A major breakthrough came with an electron crystallographic reconstruction of a 7.5-Å, three-dimensional map of a truncated Cx43 gap junction channel (Unger et al., 1999). This confirmed the presence of four membrane-spanning α-helices in each subunit with one exposed to the pore along its entire length, and a second contributing at the cytoplasmic mouth where the pore widens. However, the limited resolution of this map does not allow assignment of specific transmembrane domains to the helices, nor the identification of the nature of the residues that line the pore. This presents a major limitation to understanding the basis of selectivity in these unique channels.

As an effective alternative to the determination of structure by physical methods, the substituted cysteine accessibility method (SCAM) has been used to identify pore-lining residues for many ion channels (in Karlin and Akabas, 1998). Cysteine is substituted for one amino acid at a time in protein domains that are likely to face the channel lumen. Channel conductance is then monitored in the presence of aqueous thiol reagents that do not partition into the bilayer. A change in conductance is used as an indication that the substituted cysteine lines the pore.

In contrast to most other channels, no pharmacology exists to suggest which region of connexins contributes to the pore, other than the general observation that the third transmembrane domain has an amphipathic nature (Milks et al., 1988). A few sites have been implicated as pore-lining sites based on changes in channel properties in response to mutagenesis (E42 in the first extracellular loop, D2 on the NH_2 terminus [Oh et al., 1999], and S26 in M1 of Cx32 [Oh et al., 1997]). However, caution needs to be used interpreting such data, as mutations at sites significantly removed from the pore could still affect protein conformation and channel properties indirectly.

Some partial SCAM analyses have been applied to two of the four transmembrane domains of connexin hemichannels expressed in single oocytes, implicating M1 as a major pore-lining domain (Zhou et al., 1997). However, results from hemichannels should not be automatically extrapolated to whole channels, as differences in their permeability, conductance, and gating properties that are likely to reflect structural differences have been reported (Castro et al., 1999).

We avoid any preconceptions in the current paper by directly testing intact gap junctions and probing all four transmembrane domains. However, probing of the intact channel requires access of the thiol reagent to the cytoplasmic opening in an intact cell pair through an environment that is highly reducing. Passive perfusion through whole cell patch clamps was inadequate for this purpose, which required active perfusion of the cytoplasm. This was achieved by development of a paired oocyte perfusion system that allowed recording of junctional coupling during the perfusion process (Fig. 1). Also, an irreversible thiol blocker of sufficient size was required as the gap junction pore is large and permeable to glutathione, which is abundant in the intact cell, and capable of displacing reversible reagents from reactive cysteines. A biotinylated form of an irreversible maleimide reagent (maleimidobutyryl biocytin [MBB]) met these requirements, and provided a detailed map of the pore lining segments of gap junction channels composed of Cx32.

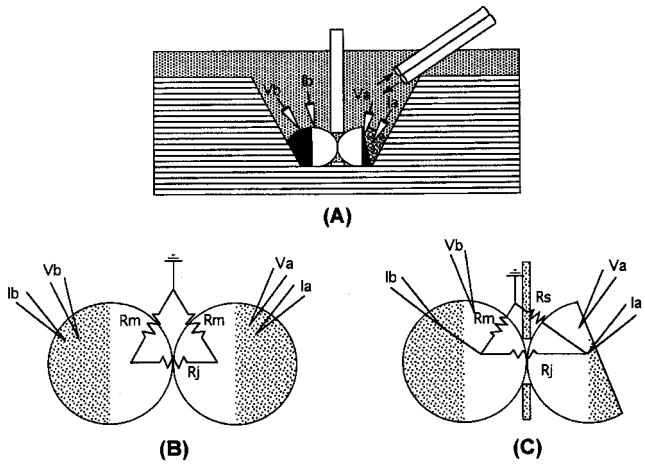

Figure 1. **Schematic representation of the dual oocyte perfusion apparatus that allows both cytoplasmic access to gap junction channels and monitoring of intercellular conductance.** The chambers, designed by F. Cao, B.J. Nicholson, and G. Nottingham (Cao, 1997), are assembled from two halves to form compartments that remain separated by a thin coverslip with a small (0.7-mm diam) hole drilled centrally (A). Oocytes, in 600 μl of L15 media per compartment, establish coupling through the hole in the coverslip, with which the oocyte membrane forms a low resistance seal. During perfusion experiments, one oocyte is cut open with fine dissecting scissors, and at this time, the seal resistance replaces the membrane resistance of the open cell as shown in the equivalent circuit (B and C).

Results

Functional analysis of cysteine substitution mutants

The initial strategy involved accessibility tests over at least one helical rotation in each transmembrane domain. Analysis of reactive regions was then expanded, in most cases to include sites at least one helical rotation above and below the identified reactive site. Cx32 was chosen as the target of our work because it readily forms functional channels in *Xenopus* oocytes, and does not pair with the endogenous *Xenopus* Cx38. Ultimately, cysteine substitutions were made at 48 sites, only three of which (W77C, W133C, and T134C) resulted in nonfunctional channels (Fig. 2, crosses). These were predicted to be located at the extracellular boundary of M2 and the intracellular boundary of M3. Based on the aromatic nature of two of the three sites, they could play critical roles in defining the position of the transmembrane helices (Mall et al., 2000).

36 of the remaining 45 functional mutants formed channels with minimal changes from the wild-type gating profile (Fig. 3, A–C). This property had been shown to be very sensitive to structural disruption of membrane-spanning regions of the protein (Suchyna et al., 1993; Skerrett et al., 1999). Hence, these mutants were considered valid candidates for probing cysteine accessibility in the native open state of the channel. The nine remaining cysteine substitutions showed modified properties (discussed below), indicating that the native channel structure had been perturbed in some manner.

Special cases

"Reverse-gating" mutants. Seven cysteine substitution mutants (Fig. 2, bold circles), including four clustered in M1, formed functional channels with similar aberrant gating responses to transjunctional voltage (Vj). Although currents

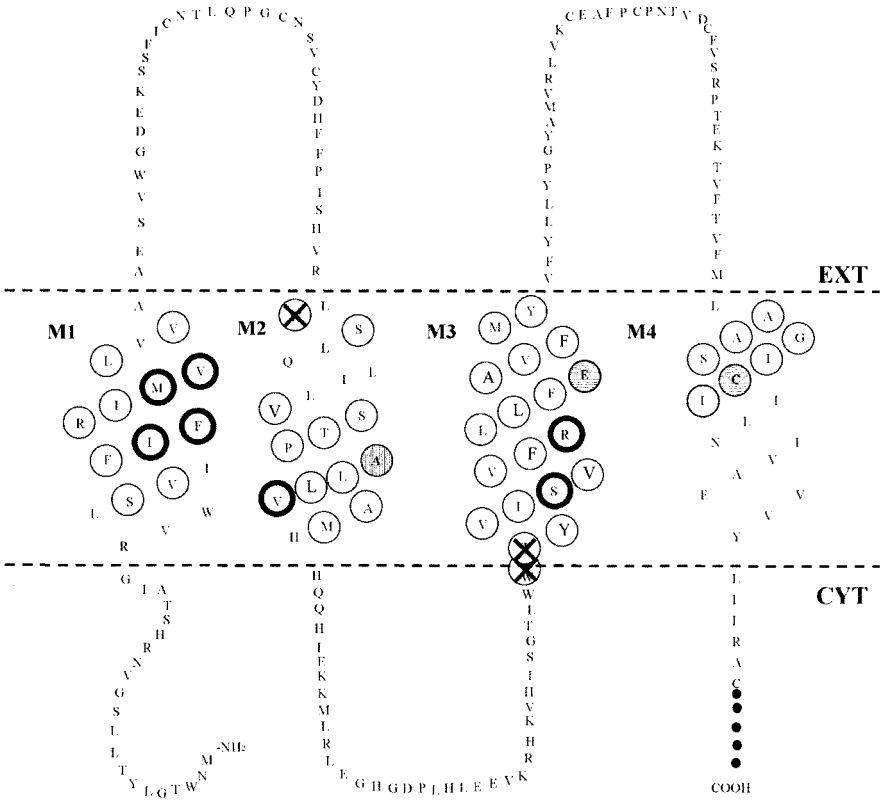

Figure 2. **Membrane topology of Cx32 showing all sites mutated to cysteine and analyzed in the current study.** Cysteine substitutions were made at the indicated sites using overlapping PCR. Nonfunctional mutants are indicated with an "X." At seven sites, cysteine substitution resulted in functional channels with a reverse-gating response to voltage (bold circles). Other sites where cysteine substitution altered channel properties (shaded circles) include A88 in M2, where cysteine substitution appears to induce hemichannel formation, and E146 in M3, where cysteine substitution results in a disulfide bond with C201 in M4 (Fig. 3, E and F). The topological plot is modified from Milks et al. (1988) to accommodate the empirical data demonstrating this proximity of E146 and C201. Extension of transmembrane spans beyond the margins shown here would be required for helices that are significantly tilted from the normal to the bilayer (helices C and D in Unger et al. [1999], corresponding to M3 and M4; Fig. 9).

could not be recorded from homotypic pairings of these mutants, heterotypic pairings with wtCx32 revealed strongly rectifying channels where junctional currents increased in response to positive Vj relative to the mutant (Fig. 3 D, traces for Cx32M34C). Given the well-characterized gating response of wtCx32 (Barrio et al., 1991), this behavior can be explained if the mutant hemichannels are closed at Vj = 0, and open on application of positive Vj. This also explains the failure to observe homotypic mutant channels, as both hemichannels would be closed at Vj = 0, and one or the other would remain closed with increasing Vj of either polarity. This phenotype, which we term "reverse gating," has been reported for other connexin mutants (Suchyna et al., 1993; Oh et al., 1999). Ultimately linked to a relative stabilization of the closed state at resting potentials, reverse gating could arise by different mechanisms, such as a shift in the voltage response along the Vj axis (e.g., the Cx32 mutants here), or an inversion of the gating response (Cx26P87L; Suchyna et al., 1993). Although the results of SCAM analysis on these reverse-gating channels are presented below, their reactivity only reflects accessibility in a closed state of the channel, as the reagent was applied in the absence of Vj (0 mV).

Cx32E146C. Although this mutant (Fig. 2, shaded residue in M3) failed to form functional channels homotypically or heterotypically with wtCx32, perfusion of the oocytes with 5 mM of the reducing agent DTT revealed wt junctional currents. Intercellular currents increased by an average of 2.3 ± 1.6 μS (± SEM; $n = 5$) over 20 min, compared to only 0.46 ± 0.3 μS (± SEM; $n = 5$) for uninjected oocyte pairs. A sample experiment is shown in Fig. 3 F. These results suggest that the introduced cysteine at position 146 is involved in a disulfide bond that locks the channel in a closed state that is reversed on reduction of the disulfide. Within the membrane-spanning region of Cx32, two possibilities for disulfide formation exist: (1) between the introduced cysteines in the M3 domains of adjacent subunits, or (2) with the only endogenous cysteine, C201, in M4 of the same subunit. The absence of dimers of Cx32E146C when examined in nonreducing SDS gels argued against the first possibility. However, consistent with the second possibility, the failure of E146C to form functional channels under nonreducing conditions was rescued by a second site mutant removing the endogenous cysteine in M4 (C201S). This double mutant (Cx32 E146C, C201S) had properties very similar to those of wild-type Cx32 (Fig. 3 E).

This empirical demonstration of disulfide formation between E146 in M3 and C201 (Fig. 2, shaded residue in M4) indicates that the β-carbons of these two residues must come within 4.6 Å in the closed channel. A slight revision of the connexin membrane topology (Fig. 2) originally proposed by Milks et al. (1988) was imposed in order to align these residues. However, the assignment shown remains consistent with precedents in other membrane proteins, and reasonable physical properties that dictate the location of membrane segments (Fig. 2, legend).

Cx32A88C. Under normal conditions, injection of RNA encoding Cx32A88C (Fig. 2, shaded residue in M2) was lethal to the oocytes. Before lysis, an outward membrane conductance (mean = 92 μS [$n = 3$] at +60 mV) that activated around −20 mV could be recorded. This was over 10-fold higher than the transmembrane conductance of wtCx32-expressing oocytes (8 μS at +60 mV [$n = 6$], activating around +30 mV). It was also similar in characteristics to those currents ascribed to open hemichannels in oocytes

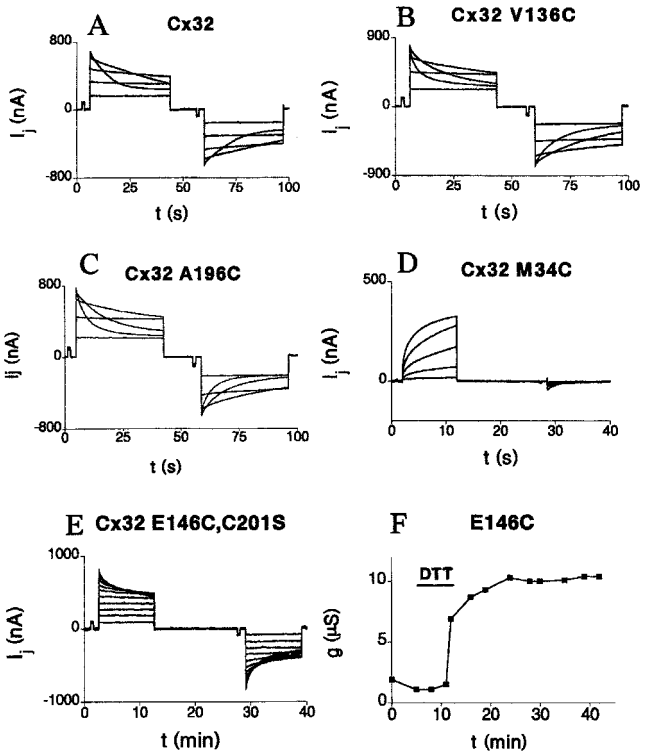

Figure 3. **Transjunctional currents recorded from paired *Xenopus* oocytes expressing wtCx32 and several representative cysteine substitution mutants.** Oocytes expressing mutants V136C (B), A196C (C), and E146CC201S (E) were paired homotypically (mutant/mutant), and showed gating responses minimally modified from wild-type Cx32 (A). Note that the E146C mutant alone was nonfunctional, and currents could only be recorded for the double mutant or after DTT perfusion of the single mutant (F). (D) M34C was paired heterotypically with wtCx32, with positive polarity defined relative to the mutant-expressing oocyte. These channels, which are closed at rest and open in response to positive transjunctional voltages, are an example of the reverse-gating phenotype discussed in Fig. 2 and the text. In all cases, transjunctional currents were recorded from oocytes clamped at −40 mV, whereas the partner was pulsed in 20-mV increments from the same holding potential.

previously (Paul et al., 1991), including wild-type Cx32 (Castro et al., 1999). Consistent with this, these currents could be reduced by 65% by the addition of 1.8 mM Ca^{2+} in the medium (ND96; see Materials and methods). Under these conditions, the health of the oocytes was maintained and transjunctional currents resembling those of wtCx32 could be recorded between paired Cx32A88C-expressing oocytes (unpublished data).

Characterization of the assay system

Introduction of the thiol reagents into the gap junction pore required a dual oocyte perfusion apparatus that allowed access to the cytoplasmic opening of the pore, and wash-out of cytoplasmic reducing agents while maintaining electrical recording of intercellular conductance (Fig. 1 A; Cao, 1997). By restricting contact between oocyte pairs to a small hole (0.7-mm diam) in a plastic coverslip, one oocyte can be cut and perfused with a pseudo-intracellular solution (see Materials and methods) without disrupting the extracellular environment of the other. As indicated in the circuit diagrams in Fig. 1 B and C, the seal resistance, Rs (∼0.2 MΩ) between the intact oocyte membrane and the coverslip replaces the resistance of the oocyte membrane (∼1 MΩ). After an oocyte was cut and perfused, there was often a slight increase in the measured junctional conductance (Gj; 12 ± 3% of the conductance before dissection [n = 20]). This is likely to represent the inclusion of channels in the nonjunctional membrane of the intact oocyte, which may contribute to the partial loss of Vj sensitivity often seen after perfusion (Fig. 4, A and B).

The thiol reagent adopted for these studies, for reasons discussed below, was a biotinylated variant of MBB (537 D; Fig. 5 A). To ensure access to the junctions in the perfused system, Cx32 was immunoprecipitated after perfusion with MBB, and reactivity assessed by streptavidin Western blot. Detection of a strong band, not present in water-injected oocytes, which co-migrated with radiolabeled Cx32 (Fig. 5 B), confirmed the efficient reaction of MBB with the endogenous cytoplasmic cysteines of Cx32. The lower band is likely to represent slight degradation of Cx32, whereas the bands detected at 50–60 kD and 90 kD are consistent with the di- and trimeric aggregated forms of Cx32 reported by Henderson et al. (1979). The latter are more evident with the more sensitive avidin detection system than in the radiolabeled sample (Fig. 5 B, compare left two lanes).

Mapping of accessible residues

Several stringent criteria were applied for inclusion of perfused pairs in the database (see Materials and methods; dual

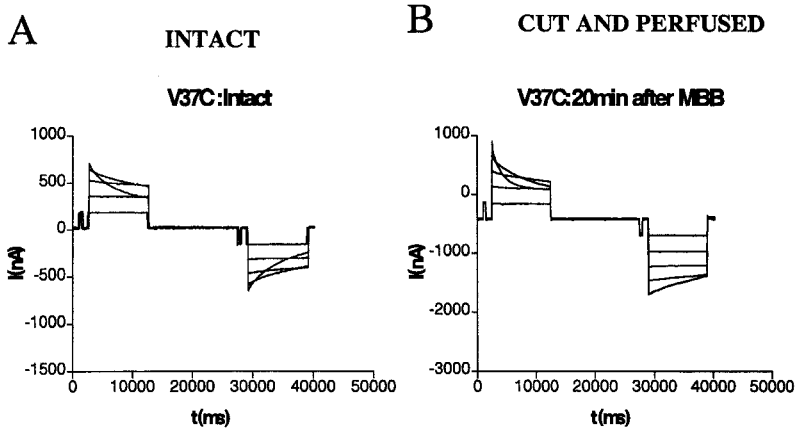

Figure 4. **Transjunctional currents recorded from paired Xenopus oocytes expressing Cx32V37C show minimal changes on perfusion.** Oocytes were paired homotypically (mutant/mutant) in the perfusion chamber, and voltage sensitivity of the junctions was assessed in the intact (A) and perfused (B) configuration. Junctional currents were altered only slightly after perfusion. Transjunctional currents were recorded from the intact oocyte clamped at −20 mV, whereas the partner was pulsed in 20-mV increments from the same holding potential.

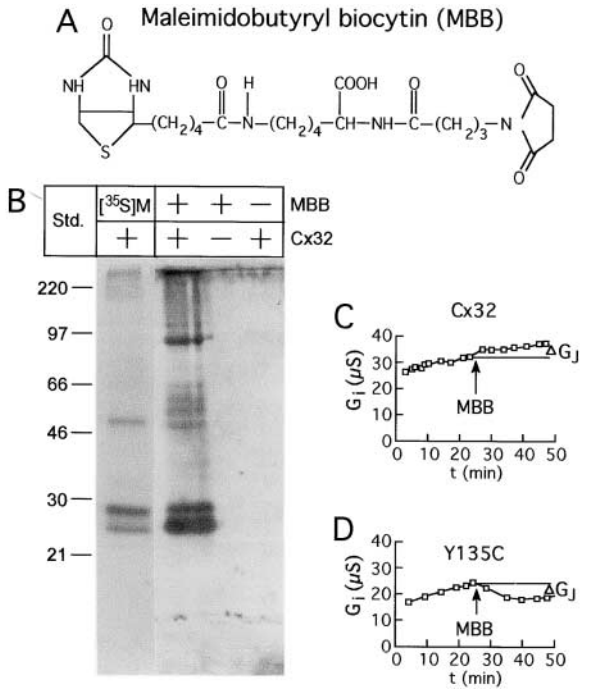

Figure 5. **Structure of the thiol reagent maleimidobutyryl biocytin (MBB), and detection of its reactivity with Cx32 in the perfusion chamber.** (A) Irreversible reaction occurs between the SH group of a cysteine and the maleimide ring, with the biotin moiety providing easy detection. (B) Biochemical determination that MBB reacts with Cx32 in the dual-oocyte perfusion system. Radiolabeled Cx32, immunoprecipitated from intact oocytes, shows a full-length and partially degraded form just below the 30-kD marker, and an aggregated dimer at ~50 kD (left lane). Cx32 detected by avidin blot after intracellular perfusion of a paired oocyte with 1 mM MBB and immunoprecipitation of Cx32 (second lane from left) reveals the same bands, although the increased sensitivity of avidin detection revealed additional aggregated forms, both dimeric (50–60 kD) and trimeric (~90 kD). No protein is detected for noninjected oocytes exposed to MBB or for perfused Cx32-injected oocytes not exposed to MBB (left two lanes). (C and D) Changes in junctional conductance (Gj) during typical SCAM experiments. In most cases, conductance increased steadily before and after addition of the reagent as shown for wtCx32 (C). In cases where a substituted cysteine was accessible, a decrease in conductance occurred after the addition of MBB, as shown for Cx32Y135C (D). The effect of MBB on each oocyte pair was determined by comparison of the conductance immediately before addition of the reagent, to that 20 min after its application (ΔGj).

oocyte perfusion). For all experiments meeting these criteria, a conductance change (ΔGj) was calculated based on the measurement of Gj immediately before, and 20 min after, application of the reagent. Fig. 5 (C and D) shows changes in junctional conductance over time for wtCx32 and Cx32Y135C, a reactive cysteine mutant. In most cases, conductance increased before and after application of the reagent, presumably the result of insertion or activation of new channels during the assay. Hence, for wtCx32 and the nonreactive cysteine mutants, the mean conductance increase after addition of MBB was 18 ± 12% (n = 10) and 9 ± 8% (n = 141), respectively (Fig. 6). Sites were deemed accessible (or reactive) if the average conductance change after MBB addition (seen in >50% of all experiments) was significantly different to that of wt Cx32 ($P < 0.04$). All accessible sites identified here showed a drop in conductance, although in some cases, like A147C, this was only slight (~2%). However, this represented a difference of ~20% in comparison to Cx32 (+18%), and was highly significant. The average level of block compared to wild type at all accessible sites (~30%) was somewhat lower than typically reported for other channels (AChR; Akabas et al., 1994), presumably reflecting the large pore size of gap junction channels, ranging from <15 Å in diameter at the extracellular end of the pore to 40 Å at the cytoplasmic end (Unger et al., 1999).

Mutant channels were generally studied in both homotypic (both paired oocytes expressing the mutant connexin) and heterotypic configurations (mutant-expressing oocyte paired with an oocyte expressing wtCx32). Although heterotypic pairs often yielded higher conductances, results never differed significantly from those of homotypic pairs. For instance, application of MBB to the reactive Cx32L144C mutant caused a decrease in conductance of 13 ± 8% (n = 6) in homotypic pairs. In comparison, application to the wild-type or mutant-expressing oocyte of a heterotypic Cx32/Cx32L144C pair decreased conductance by 11 ± 5% (n = 4) or 9 ± 2% (n = 4), respectively. This demonstrates that the reagent is capable of permeating the length of the pore, as the reaction with the site in the first half of the gap junction channel (i.e., MBB applied to the mutant side) is comparable to that in the second half of the channel (i.e., MBB applied on the wt side).

Figs. 6 and 7 summarize conductance changes for all cysteine mutants tested in perfused and intact configurations (see below), respectively. Filled bars indicate residues that showed a significant drop in conductance and also displayed wild-type gating properties. In the perfused system (Fig. 6), block at most "reactive sites" (black bars) was seen in 60–100% of experiments (numbers to the right of each bar), and the mean conductance change induced by MBB differed from that of wt Cx32 at a significance level of $P < 0.01$ (t test). Four sites (Fig. 6, gray bars in M2 and M3) were termed "weakly reactive" and showed a lower significance level ($0.01 < P < 0.04$) with block observed in only 50% of experiments. Nonreactive sites (open bars) showed conductance drops only 20% of the time on average. Bolded open bars in Fig. 6 indicate sites where cysteine substitution altered the gating properties of the channel, such that accessibility was tested only in the closed state.

The majority of reactive residues occur in M3, where they span five rotations of the α-helix with a periodicity of ~3, defining a diagonal stripe on one face of the helix at ~15° to the helix axis (see Fig. 8). This pattern seemed to break down in the last 1 to 2 turns towards the extracellular surface of the membrane (reactivity at A147C and F149C and Y151C [weak]), suggesting a disruption to the helix at this point (see Discussion). A complete accessibility map of M3 in the open conformation was prevented, as cysteine substitution at R142 and S138 induced a reversed-gating phenotype, and thus could only be tested for accessibility in a closed state of the channel. However, it is notable that S138C, which lies on the reactive surface of the M3 helix in the open state (Fig. 8), was significantly reactive in the closed state (Fig. 6, bolded open bar in M3).

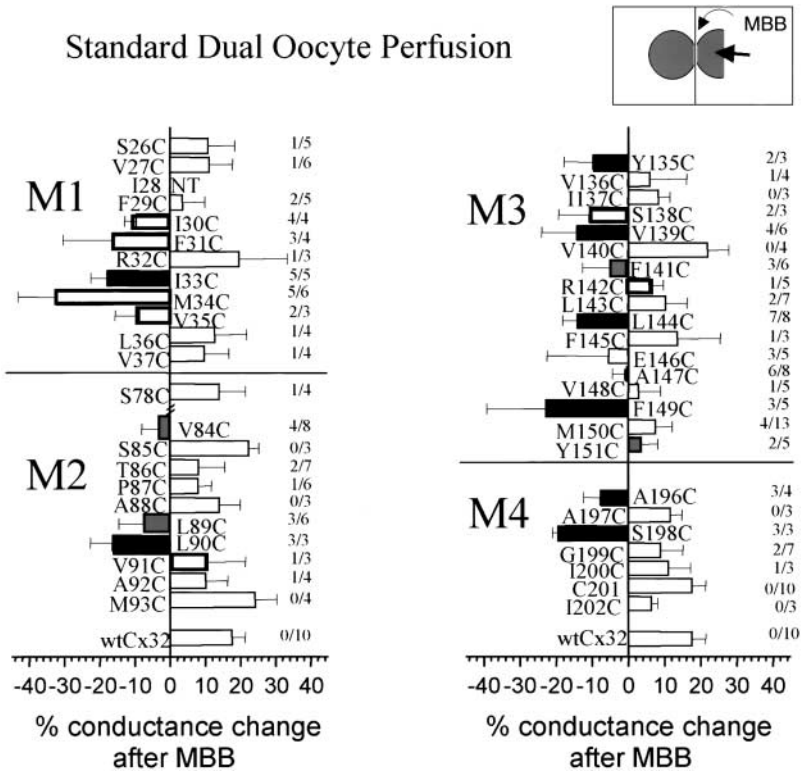

Figure 6. **Mean percent changes in conductance after MBB perfusion.** For Cx32 and the majority of cysteine substitution mutants, a small increase in conductance occurs after addition of the reagent, which represents a continuation of the trend in conductance before the application of MBB (open bars). A significant decrease in conductance compared to wt was observed after application of MBB to a number of cysteine substitution mutants (black bars, $P < 0.01$; shaded bars, $0.01 < P < 0.05$). In all of these cases, block was also observed in ≥50% of perfusions (>60% for black bars). Bolded open bars indicate sites where cysteine substitution altered the gating properties of the channel. Hence, reactivity does not necessarily infer that the native amino acid lies in an accessible position. Error bars represent SEM. Numbers adjacent to the bars indicate the number of experiments where conductance was reduced versus the number of experiments conducted.

In M1, four of the five reactive sites displayed a reverse-gating phenotype (I30C, F31C, M34C, and V35C) so that their accessibility was only demonstrated in a closed state of the channel (Fig. 6, bolded open bars). A noncysteine substitution at one of the sites, M34S, also induced a reverse-gating phenotype, but was nonreactive (unpublished data), demonstrating that reactivity of mutants with this phenotype was due to access to the site itself and not to altered accessibility of the endogenous cysteines. Of the seven sites in M1 where cysteine substitution did not greatly alter the response of channels to Vj, only I33C in the mid-portion of the M1 helix was reactive.

Three reactive sites were identified in M2. L90C, closest to the cytoplasmic end of the protein, was strongly reactive and L89C and V84C were weakly reactive. The reactive residues lie on either side of the conserved proline at position 87, which has been implicated in voltage gating of Cx26 (Suchyna et al., 1993) and Cx32 channels (Ri et al., 1999). Although the P87C substitution itself does not affect gating in Cx32, the lack of reactivity of this mutant is difficult to interpret. Given the unique properties of proline, this substitution is likely to have modified the local conformation of this part of the protein. In M4 six sites were tested in addition to the native cysteine at position 201. Only A196C and S198C, at the extracellular end of M4, were reactive.

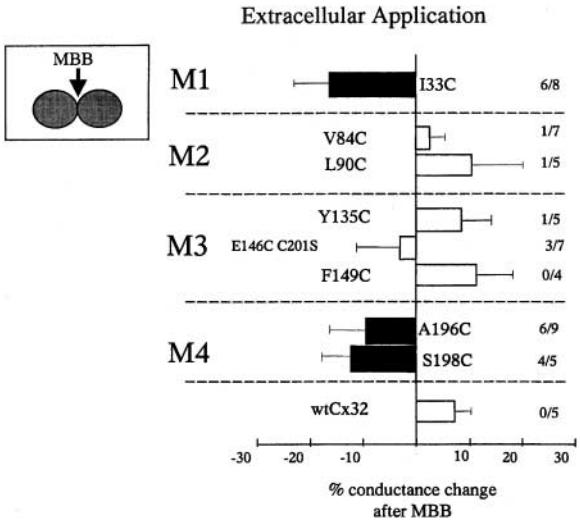

Figure 7. **Changes in conductance after extracellular MBB application to intact oocyte pairs where access to the pore was not possible.** As in the perfusion experiments in Fig. 6, wtCx32 and cysteine substitution mutants in M2 and M3 continued to show small increases in conductance after addition of the reagent. In contrast, significant decreases in conductance compared to wt ($P \leq 0.05$; *t* test) were observed after application of MBB to a number of cysteine substitution mutants in M1 and M4 (filled bars). In all of these cases, block was also observed in >50% of perfusions. Reactivity suggests that the designated cysteines lie within an MBB-accessible environment, continuous with the extracellular space but not in the pore. Data are presented in the same format as Fig. 6.

Accessibility of nonpore-lining cysteines

A surprising finding in our SCAM analysis was that reactivity was not restricted to a single domain, but was found, to a limited extent, in all four transmembrane helices. This was far more extensive than would have been expected from the gap junction structure of Unger et al. (1999) that suggested no more than 2 helices are exposed to the pore. However, several reports on other channels (Williams and Akabas, 1999) have demonstrated that access to cysteines can occur through aqueous "crevices" within the membrane, or be-

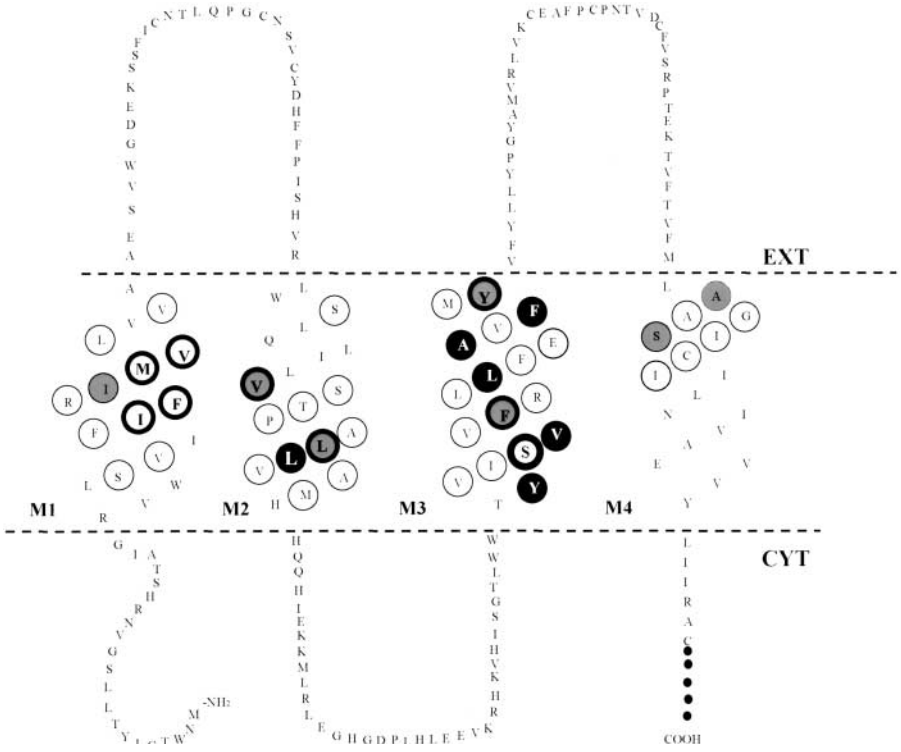

Figure 8. **Position of all significantly reactive cysteines in Cx32.** Solid filled circles in M2 and M3 indicate sites where channel block by MBB was highly significant ($P < 0.01$), whereas boldly circled residues with lighter shading (V84 and L89 in M2; F141 and Y151 in M3) showed conductance changes that were slightly less significant ($0.01 < P < 0.05$). Lightly shaded residues in M1 (I33) and M4 (A196 and S198) showed block in response to extracellular MBB application, and are not thought to line the pore. Boldly circled open sites indicate reactive positions where cysteine substitution induced reversed gating. Reactivity of these residues suggests that they are accessible in the closed state, but not necessarily in the native, open conformation.

tween transmembrane helices. To test for reactivity via extracellular aqueous crevices we applied MBB to the medium bathing paired oocytes. Without perfusion of the cytoplasm, access to the pore was excluded in this configuration, as MBB is membrane impermeable (Zhou et al., 1997). Unfortunately, it was not possible to perform similar tests from the cytoplasmic surface without including access to the pore.

The effect of extracellularly applied MBB on junctional conductance was assessed for 8 cysteine mutants (Fig. 7), all of which displayed normal gating properties and were reactive in the perfused configuration. Of these, all residues in M1 and M4 that were reactive in the open state (I33C, S198C, and A196C) were similarly sensitive to extracellular application of the reagent, and could be eliminated as potential pore-lining sites (Fig. 7, filled bars). Access of the maleimide moietey of MBB to these sites could occur either through specific extracellular aqueous crevices in the membrane, or by intrusion of the uncharged end of MBB (~10 Å in length) into the lipid bilayer, with the biotin moietey remaining at the surface. This may explain the increased reactivity we observe 1–2 turns into the bilayer (Fig. 8). Reactivity within the lipid bilayer itself could be possible if the reaction between the thiol and maleimide groups proceeds through a free-radical intermediate, but would be unlikely if it proceeds through the anionic form, S^-.

Lack of reactivity to extracellularly applied MBB for sites in M2 and M3, including those close to the extracellular surface (e.g., F149C), is consistent with their direct contribution to the pore, and also supports previous reports that MBB does not cross the bilayer (Zhou et al., 1997). The location of all reactive residues, including those accessible from the extracellular space (shaded circles in M1 and M4) as well as the cytoplasmic face (bold/shaded circles in M2 and M3), is clarified with the topology plot in Fig. 8.

Partial block by MBB is due to partial block of all channels

As reported in the SCAM analysis of hemichannels using the same reagent (Zhou et al., 1997), we consistently found only partial channel block at all reactive sites, ranging from 17 to 44% (average 30%) when normalized to wt Cx32. This could arise from closure of a subset of channels, or a partial occlusion of all channels. We found that the partial nature of the channel block was not affected by over fivefold changes in MBB concentration (at V139C, a $-21.8 \pm 6.0\%$ conductance drop was reported at 0.2 mM MBB, and $-14.2 \pm 9.8\%$ at 1 mM MBB). Hence, it is likely to reflect partial block of all channels rather than complete block of some channels. This is consistent with the size of MBB (537 D) compared to the empirical cut-off limit for Cx32 channels (>790 D; Nicholson et al., 2000), and the observation by Zhou et al., (1997), that reduction in the size of the reagent resulted in reduced block of connexin hemichannels. Conversely, we attempted the use of a larger reagent (Alexa 594-maleimide; D = 950). This also resulted in lower levels of block (11% [$n = 5$]) compared to MBB (18%) at the V139 site (unpublished data). Presumably, any increase in blockage of individual channels was offset by decreased access to the pore (compare the MTSEA and MTSET block of the AChR; Akabas et al., 1994).

Discussion

Mapping the pore and other domains

Of the 49 cysteine substitutions investigated here, 39 formed channels with wild-type properties. To our initial surprise, the 11 sites that showed significant channel block in response to MBB were scattered on all four transmembrane helices. However, all sites in M1 (I33C) and M4

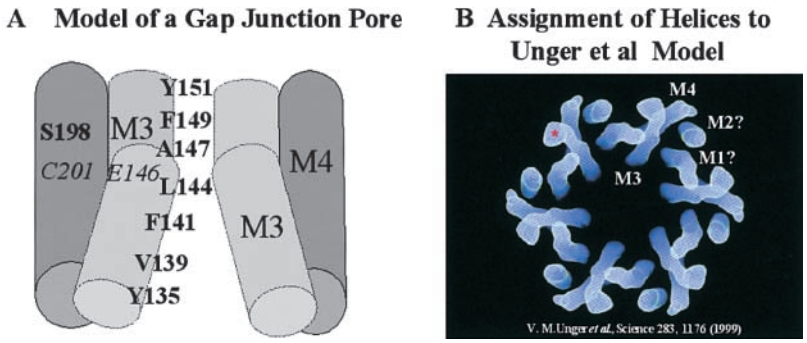

Figure 9. **Models of the pore-lining helices of connexins showing reactive sites and the proposed assignment of helices in the gap junction structure.** (A) Reactive sites span the length of the M3 helix, which appears to lose its helical periodicity at its extracellular end (displayed as a "break" in the helix). The positioning of M4 is based on the observation that a disulfide bond is capable of forming between C201 in M4, and a substituted cysteine at position 146 in M3. (B) Helical assignments to the gap junction structure of Unger et al. (1999). The main pore-lining helix (M3) is assigned with certainty based on the accessibility of M3 residues in both open and closed channels. The M4 assignment is based on evidence for disulfide formation. There is less certainty regarding the assignments of M1 and M2. It has been proposed (see Discussion; Helical assignments) that the structure shown in B is in the closed state, where M1 would contribute to the pore at the widened cytoplasmic mouth. However, our data indicate that M2 would contribute to the pore mouth in the open state.

(A196C and S198C) that showed reactivity in the open state of the channel appeared not to lie in the pore, as they were accessible from the extracellular medium. Hence, M2 and M3 emerged as the pore-lining domains for open gap junction channels composed of Cx32. The distribution of reactive sites along the length of the M3 helix implicated it as the major pore-lining segment of the gap junction channel. The pattern of reactivity in M3 is consistent with the exposure of one face of an α-helix, tilted at ~15° from the normal to the membrane. This is similar to the major pore-lining helix C in the model of Unger et al. (1999) that appears to be tilted ~10° to the pore axis. Towards the extracellular end of M3, the helical periodicity seems to break down with A147, F149, and Y151 (a weakly reactive site at the $P < 0.05$ level of significance), showing a repeat pattern more characteristic of β-sheet. This is likely to reflect a local disruption of the helix, consistent with the bend or distortion near the extracellular end of the major pore-lining C-helix in the structure of Unger et al. (1999). A similar nonhelical periodicity is observed in a distorted region of the M2 pore-lining helix of the AChR (Akabas et al., 1994). Notably, the F149C site produces one of the highest levels of block, consistent with the location of the distortion in helix C at the narrowest part of the pore.

Reactivity at V139 towards the cytoplasmic end of M3 represents a minor deviation from the expected helical periodicity. However, the adjacent S138 site lies on the same face of the helix as other reactive sites, and is strongly reactive in the closed state (Figs. 6 and 8). It is likely that S138 is also exposed to the pore in the open state. Initial comparisons of reactive M3 residues in the closed and open states indicate little change in conformation at the cytoplasmic end of this helix (i.e., V139 and L144 are reactive in both open and closed states of the channel; unpublished data). The reactivity of adjacent residues in this part of M3 is not surprising, given that the cytoplasmic end of the pore is its widest dimension.

Contribution of a second helix ("B" in the Unger structure) to the wider cytoplasmic mouth of the gap junction channel is supported by the published structure (Fig. 9 B). Given that the structure imaged by Unger et al. (1999) is likely to be in a partially closed state, we have tentatively ascribed helix B as M1 in this structure because several sites in M1 are accessible in the closed state (V35C, F31C, and I30C). However, in the open state of the channel, M2 may contribute to the pore, including one strongly reactive site at L90 and two weakly reactive sites at L89 and V84. Thus, in the open and closed states of the channel, different helices may contribute to the pore. This would require major conformational changes during gating, but is not inconsistent with the large conformational changes that have been reported for other ion channels (i.e., mechanosensitive [Suknarev, 2001], and K^+ channels [Jiang et al., 2002]).

Helical assignments to the gap junction structure of Unger et al. (1999)

The mapping of specific residues that contribute to the pore lining of gap junctions, as well as a site of interaction between helices M3 and M4, allows us to make the first empirically based helical assignments to the 7.5-Å map of the gap junction channel (Unger et al., 1999). In making these assignments, two caveats must be kept in mind. First, site mapping and structure determination were performed on different connexins (Cx32 and 43, respectively), although the conservation of the transmembrane domains of connexins suggests a general conservation of structure. Second, although we have mostly mapped accessibility in the open state, junctions for structural analysis were isolated in the presence of an uncoupling agent (oleamide) with the intent of stabilizing a closed form of the channel. This could not be confirmed functionally, but when amino acid side chains are factored into the low resolution structure, the pore diameter would be significantly reduced to ~6 Å. Although consistent with a partially closed state of the pore, it would still be expected to conduct ions and mediate coupling.

Our assignment of M3 as the major pore-lining helix C in the structure is not dependent on the state of the channel, as S138 (Fig. 6), V139, and L144 (unpublished data) were all found to be accessible in the closed channel. The inter-helical interaction between the nonpore-lining face of M3 and M4 (based on disulfide formation between E146C and C201 in the closed state) implicates M4 as the D-helix in the Unger et al. structure (Fig. 9, A and B). Both C and D helices in the structure are significantly tilted, and would require more residues to cross the bilayer. Consistent with this, both M3 and M4 could be extended by 6 to 7 amino acids at their extracellular end and 3 to 6 amino acids at

their cytoplasmic ends based on the distribution of nonpolar residues. Assignment of transmembrane domains to the A and B helices in the published structure is less clear because we cannot presently differentiate between reactive sites that lie within the pore and those that may be directly accessible from the cytoplasm. In addition, given that M1 and M2 are reactive in the closed and open conformations, respectively, assignment of these two helices depends on the state of the crystallized channel at the time of isolation. We have assigned M1 to helix B in Fig. 9 B with the assumption that the pore is in a partially closed state.

Comparison of intercellular gap junctions and hemichannels

A comparison of the data presented here with the initial SCAM study of Zhou et al. (1997) provides a preliminary assessment of structural differences between hemi- and gap junction channels. Comparison of the results from hemichannel analysis of a chimera of Cx32 with E1 derived from Cx43 (because wtCx32 does not form stable hemichannels) is consistent with the assumption that the transmembrane structure of Cx32 is not dramatically different in hemi- and intact channels. Most of the reactive sites in M1 identified in the hemichannels were also reactive in the intercellular channel (F31, I33, and M34). However, all of these sites were either exposed in the closed state of the gap junction channel or located within an extracellularly accessible environment. Although they suggest similar conformations of M1 in hemi- and whole channels, they provide no insight into the structure of the open channel.

Within M3, the major pore-lining segment identified here, reactivity patterns between hemichannels and intercellular channels were more divergent. Of the reactive hemichannel sites (S138, E146C, and M150C), only S138 was reactive in gap junctions. This could only be demonstrated in the closed state, although as noted above, it is likely to also be exposed in the open channel, as is the adjacent V139 site. Although neither of the other two sites showed significant reactivity, adjacent sites were reactive in the intercellular channel (A147 and F149). These initial comparisons suggest that docking may subtly alter the pore-lining region of gap junction channels without inducing major conformational changes in M1. This is consistent with previous reports that channel conductance and dye permeability differ between Cx32 hemi- and intercellular channels. For instance, Castro et al. (1999) observed a single channel conductance of 17 pS for Cx32 hemichannels; significantly smaller than the 100 pS that would be predicted based on whole-channel properties. Preliminary data in our lab also indicates that the molecular size cut-off for dye permeability of hemichannels is significantly lower than that for whole channels composed of the same connexin (Weber, P., personal communication).

Pore structure and its implications for selectivity

Ironically, although Milks et al. (1988) proposed the same assignment of M3 as the major pore-lining helix 14 years ago that we have now demonstrated empirically, the logic behind their prediction appears to have been erroneous because the residues identified as pore lining in both M3 and M2 are hydrophobic in nature. Although it is not unusual for hydrophobic residues to face the pore of ion channels, where they have been proposed to enhance ion flux by minimizing strong binding of permeants (Doyle et al., 1998), a complete lack of hydrophilic sites is surprising. Two of the three polar residues in M3 (S138 [reactive] and R142 [unreactive]) could only be tested in the closed state. However, given preliminary indications that little conformational change occurs at this end of M3 during gating (see above), it seems likely that S138 is exposed to the open pore, and R142 is not. The charged arginine could be accommodated in the lipid bilayer by salt bridging (possibly E208 in M4) or by pKa shift, both of which have been reported in other membrane proteins. Alternatively, there is ample documentation of charged residues being buried in the hydrophobic interior of proteins (Kajander et al., 2000), often as a means of destabilizing a structure that must undergo dynamic events such as gating. The other polar residue of M3, E146, showed variable MBB reactivity that was not significantly different to wtCx32 ($P > 0.09$). This reactivity also could be fully accounted for by extracellular access of MBB, rather than exposure to the pore (compare Figs. 6 and 7).

Although Cx32 channels are mildly anion selective (Suchyna et al., 1999), most gap junction channels favor the transfer of positively charged dyes and ions by a factor of 2 to 5 (Veenstra, 1996). This has been explained by the presence of a fixed negative charge within the pore (either in the transmembrane [Brink and Dewey, 1980] or extracellular domains [Trexler et al., 2000]), or at its mouth (Banach et al., 2000). However, in other ion channels, charge selectivity is not achieved by the presence of charges in the pore lining, as this leads to tight binding that is incompatible with rapid flux. Instead, oriented dipoles or polar interactions defining chelation chemistry have defined selectivity (Doyle et al., 1998). The same appears likely to be true in gap junction channels. It is possible, in this case, that the close location of charged residues to the pore without actually being accessible to our reagents could influence the local electrical field experienced by a permeant, creating charge selectivity in the absence of strong binding.

Of greater importance to the gap junction field than ion selectivity has been the recent demonstrations of selective permeabilities for metabolites between connexins. Despite almost identical permeabilities to anionic dyes, Cx43 and Cx32 gap junctions show over 100-fold differences in their permeability to anionic ATP and ADP (Goldberg et al., 1999). Bevans et al. (1998) also reported that changes in connexin composition in hemichannels reconstituted in liposomes can also impart even more subtle selectivity between cGMP and cAMP. These observations suggest distinctions between natural permeants of gap junctions that cannot be explained in terms of size and charge alone, but presumably involve differential binding to the pore.

In this regard, a comparison of the pore lining residues identified here with corresponding sites in several connexins is shown in Fig. 10. Aromatic residues at either end of M3 are highly conserved, and possibly contribute to the general cation preference displayed by most gap junction channels. Properties of corresponding residues in other connexins are generally conserved, suggesting that subtle differences in res-

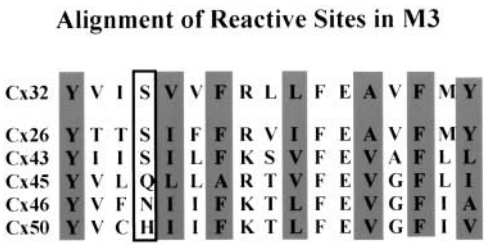

Figure 10. **Aligned amino acid sequences for the third transmembrane domain of Cx32 and several other connexins.** Highlighted residues indicate pore-lining residues in Cx32 and their corresponding sites in other characterized connexins (open-boxed site only tested in the closed state). The periodicity in the NH_2-terminal two-thirds of M3 suggests α-helix, but this breaks down at the COOH-terminal end. Many sites are strictly conserved, whereas others show relatively minor changes despite reports of significant differences in permeability between connexins. This suggests that subtle differences in residue length or branching may define the affinity of binding sites within the pore.

idue length or branch location could play a major role in defining the affinity of binding sites within the pore. The identification of pore-lining residues in Cx32 presented here provides the first comprehensive platform from which structural elements determining gap junction channel permeation can be sought. Unlike their classical ion channel counterparts, gap junction channels are likely to interact in different ways with molecular permeants and ions that will probably include weak binding chemistry involving hydrophobic, van der Waals, and induced dipole interactions.

Materials and methods

Preparation of cysteine mutants and cRNA

Rat Cx32 (Paul et al., 1986) was cloned into the EcoRI site of PGem7zf (+) (Promega). Mutants were made by site-directed mutagenesis using overlap extension by PCR as described by Ho et al. (1989), using PWO DNA polymerase (Boehringer) over 30 cycles in a Programmable Thermal Controller (model PTC-100; MJ Research, Inc.). Primer length was 19–21 bases for universal primers and 21–24 bases for mutant primers. Sequencing across the entire coding region of each clone was performed using the fmol DNA Cycle Sequencing System (Promega) with γ-[^{32}P]ATP from PerkinElmer and separation on 6% Long Ranger® gels (FMC Corporation), or by the CAMBI Nucleic Acid Facility (SUNY at Buffalo, Buffalo, NY). cRNA was prepared using mMessage mMachine™ RNA kits (Ambion) or Ampliscribe™ SP6 High Yield Transcription kits (EPICENTRE).

Expression and recording from oocytes

Intercellular currents were recorded from paired *Xenopus* oocytes coinjected with 4–20 ng connexin RNA mixed with 4 ng antisense oligonucleotide directed against nucleotides 327–353 of the endogenous *Xenopus* Cx38 (Barrio et al., 1991) as described previously (Skerrett et al., 2000). With the exception of A88C-injected cells, oocytes were continuously bathed in half-strength L15 media that included 89 mM KCl, and 0.2 mM $CaCl_2$ (Sigma-Aldrich). A88C-expressing oocytes were bathed in ND96 (96 mM NaCl, 2 mM KCl, 1 mM $MgCl_2$, 1.8 mM $CaCl_2$, and 5 mM Hepes, pH 7.4).

Dual oocyte perfusion

The perfusion apparatus (designed by F. Cao, B.J. Nicholson, and G. Nottingham, at State University of New York at Buffalo, Buffalo, NY; Cao, 1997) is illustrated in Fig. 1. The volume on each side of the chamber was maintained at 600 μl. Coupled oocytes made contact through a small hole in a coverslip (0.7-mm diam) that otherwise separates their extracellular environments. It was possible to use the same virtual ground circuit for both oocytes because the seal resistance between the oocyte membranes and the coverslip is <1 MΩ. Junctional conductance was measured using the dual oocyte voltage-clamp technique (using two Geneclamp amplifiers; Axon Instruments, Inc.) described in Skerrett et al. (2000), with pulses from +80 to −120 mV from a holding potential of −20 mV. Data were acquired and analyzed using PClamp6 software (Axon Instruments, Inc.). Currents were measured within the first 100 ms of the voltage pulse (instantaneous current), except in the case of mutants that displayed a reversed-gating phenotype, where Gj was calculated from the steady-state current at the end of a 1–4-s voltage pulse.

If the conductance was within a range deemed appropriate for analysis of channel block (3–50 μS), the solution in one compartment was replaced with a pseudo-intracellular solution (89 mM KCl, 2.4 mM $NaHCO_3$, 0.8 mM $MgCl_2$, 0.2 mM EGTA, and 15 mM Hepes, pH 7.4) using a peristaltic pump. The oocyte was then cut virtually in half, using fine microdissecting scissors. As shown in the equivalent circuit diagram (Fig. 1, b and c), the seal resistance between the oocyte cell membrane and the coverslip (Rs = 0.17 ± 0.04 MΩ; mean ± SEM, n = 10) replaces the membrane resistance of the cut cell. The bath was grounded on the side of the intact oocyte and junctional currents were measured with respect to the perfused cell (e.g., the intact oocyte was pulsed while the clamping current required for the perfused oocyte was recorded as the junctional current). In most cases, junctional conductance increased by <10% after the cut; however, if a dramatic (>25%) increase occurred, the pair was discarded.

Conductance was monitored at 5-min intervals for at least 20 min, and the reagent was applied to pairs that displayed a stable or progressively increasing conductance during this time. For typical perfusion experiments, 3 μl maleimidobutyryl biocytin (MBB; Calbiochem) was added from a 200-mM stock dissolved in DMSO (Sigma-Aldrich), and gently mixed by micropipette, resulting in a final concentration of 1 mM MBB. For extracellular applications of the reagent, oocytes were paired in agar wells, and MBB was added from a stock solution directly to the L15 bathing media, for a final concentration of 1 mM. Because addition of the reagent occasionally disrupted the seal, experiments were excluded from analysis if the conductance increased by >40% after addition of the reagent. Conductance was monitored at 5-min intervals for at least 20 min after addition of the reagent, and the effect of MBB was determined by comparing the conductance immediately before addition of the reagent and the conductance 20 min after application.

Biochemistry

To test whether MBB could access Cx32 in our dual oocyte perfusion system, we applied 1 mM MBB to Cx32-expressing oocytes, as described for perfusion experiments. The perfused oocyte was then rinsed thoroughly, extracted from the chambers by Pasteur pipette, and subjected to standard Cx32 immunoprecipitation protocols (for review see Skerrett et al., 2000) using an antibody to Cx32 (residues 223–244). After the samples were run on a 12.5% polyacrylamide gel and transferred for Western Blot analysis, the MBB-labeled proteins were detected using a chemiluminescent avidin detection system (Pierce Chemical Co.). To confirm the molecular weight of the MBB-labeled protein, radiolabeled Cx32 from the same batch of oocytes was run concurrently on the same 12.5% polyacrylamide gel and detected by autoradiography.

We thank Mary Merritt for technical assistance, Gary Nottingham for design and manufacture of perfusion chambers, and J.F. Smith, P. Weber, and H. Zhu for scientific discussion.

This work was supported by American Heart Association (NY State Affiliate) postdoctoral fellowships to I.M. Skerrett and G. Cymes, an International Agency for Research on Cancer (World Health Organization) postdoctoral fellowship to I.M. Skerrett, and National Institutes of Health grant no. GM555437 to B.J. Nicholson.

Submitted: 10 July 2002
Revised: 28 August 2002
Accepted: 28 August 2002

References

Akabas, M.H., C. Kaufmann, P. Archdeacon, and A. Karlin. 1994. Identification of acetylcholine receptor channel-lining residues in the entire M2 segment of the α subunit. *Neuron.* 13:919–927.

Banach, K., S.V. Ramanan, and P.R. Brink. 2000. The influence of surface charges on the conductance of the human connexin37 gap junction channel. *Biophys. J.* 78:752–760.

Barrio, L.C., T. Suchyna, T. Bargiello, L.X. Xu, R.S. Roginski, M.V. Bennett, and B.J. Nicholson 1991. Gap junctions formed by connexins 26 and 32 alone and in combination are differently affected by applied voltage. *Proc. Natl.*

Acad. Sci. USA. 88:8410–8414.

Bevans, C.G., M. Kordel, S.K. Rhee, and A.L. Harris. 1998. Isoform composition of connexin channels determines selectivity among second messengers and uncharged molecules. *J. Biol. Chem.* 273:2808–2816.

Brink, P.R., and M.M. Dewey. 1980. Evidence for fixed charge in the nexus. *Nature.* 285:101–102.

Cao, F. 1997. Gap junctions: A study of their differential permeability to fluorescent probes and their gating in response to intracellular pH. Ph.D. thesis. State University of New York at Buffalo, Buffalo, NY. 1–129.

Castro, C., J.M. Gomez-Hernandez, K. Silander, and L.C. Barrio. 1999. Altered formation of hemichannels and gap junction channels caused by C-terminal connexin-32 mutations. *J. Neurosci.* 19:3752–3760.

Doyle, D.A. J. Morais Cabral, R.A. Pfuetzner, A. Kuo, J.M. Gulbis, S.L. Cohen, B.T. Chait, and R. MacKinnon. 1998. The structure of the potassium channel: molecular basis of K+ conduction and selectivity. *Science* 280:69–77.

Eiberger, J., J. Degen, A. Romualdi, U. Deutsch, K. Willecke, and G. Söhl. 2001. Connexin genes in the mouse and human genome. *Cell Adhes. Commun.* 8:163–165.

Elfgang, C., R. Eckert, H. Lichtenberg-Fraté, A. Butterweck, O. Traub, R.A. Klein, D.F. Hüsler, and K. Willecke. 1995. Specific permeability and selective formation of gap junction channels in connexin-transfected HeLa cells. *J. Cell Biol.* 129:805–817.

Goldberg, G.S., P.D. Lampe, and B.J. Nicholson. 1999. Selective transfer of endogenous metabolites through gap junctions composed of different connexins. *Nat. Cell Biol.* 1:457–459.

Henderson, D., H. Eibl, and K. Weber. 1979. Structure and biochemistry of mouse hepatic gap junctions. *J. Mol. Biol.* 132:193–218.

Ho, S.N., R.M. Hunt, J.K. Horton, J.K. Pullen, and L.R. Pease. 1989. Site-directed mutagenesis by overlap extension using polymerase chain reaction. *Gene.* 77:51–59.

Jiang, Y., A. Lee, J. Chen, M. Cadene, B.T. Chait, and R. MacKinnon. 2002. The open pore conformation of potassium channels. *Nature.* 417:523–526.

Kajander, T., P.C. Kahn, S.H. Passila, D.C. Cohen, L. Lehtio, W. Adolfsen, J. Warwicker, U. Schell, and A. Goldman. 2000. Buried charged surface in proteins. *Structure.* 8:1203–1214.

Karlin, A., and M.H. Akabas. 1998. Substituted cysteine accessibility method. *In* Methods in Enzymology; Ion Channels. Pt. B. Vol. 293, P.M. Conn, editor. Academic Press Inc., San Diego, CA. 123–145.

Kelsell, D.P., J. Dunlop, and M.B. Hodgins. 2001. Human diseases: clues to cracking the connexin code? *Trends Cell Biol.* 11:2–6.

Mall, S., R. Broadbridge, R.P. Sharma, A.G. Lee, and J.M. East. 2000. Effects of aromatic residues at the ends of transmembrane α-helices on helix interactions with lipid bilayers. *Biochemistry*. 39:2071–2078.

Milks, L.C., N.M. Kumar, R. Houghten, N. Unwin, and N.B. Gilula. 1988. Topology of the 32-kd liver gap junction protein determined by site-directed antibody localizations. *EMBO J.* 7:2967–2975.

Nicholson, B.J., P.A. Weber, F.-L. Cao, H.-C. Chang, P. Lampe, and G. Goldberg. 2000. The molecular basis of permeability of connexins is complex and includes both size and charge. *Braz. J. Med. Biol. Res.* 33:369–378.

Oh, S., Y. Ri, M.V.L. Bennett, B. Trexler, V.K. Verselis, and T.A. Bargiello. 1997. Changes in permeability caused by connexin 32 mutations underlie X-linked Charcot-Marie-tooth disease. *Neuron* 19:927–938.

Oh, S., J.B. Rubin, M.V.L. Bennett, V.K. Verselis, and T.A. Bargiello. 1999. Molecular determinants of electrical rectification of single channel conductance in gap junctions formed by connexins 26 and 32. *J. Gen. Physiol.* 114:339–364.

Paul, D.L. 1986. Molecular cloning of cDNA for rat liver gap junction protein. *J. Cell Biol.* 103:123–124.

Paul, D.L., L. Ebihara, L.J. Takemoto, K.I. Swenson, and D.A. Goodenough. 1991. Connexin 46, a novel lens gap junction protein induces voltage-gated currents in nonjunctional plasma membrane of *Xenopus* oocytes. *J. Cell Biol.* 115:1077–1089

Phelan, P., and T.A. Starrich. 2001. Innexins get into the gap. *Bioessays.* 23:388–396.

Plum, A., G. Hallas, T. Magin, F. Dombrowski, A. Hagendorff, B. Schumacher, C. Wolpert, J. Kim, W.H. Lamers, M. Evert, et al. 2000. Unique and shared functions of different connexins in mice. *Curr. Biol.* 10:1083–1091.

Ri, Y., J.A. Ballesteros, C.K. Abrams, S. Oh, V.K. Verselis, H. Weinstein, and T.A. Bargiello. 1999. The role of a conserved proline residue in mediating conformational changes associated with voltage gating of Cx32 gap junctions. *Biophys. J.* 76:2887–2898.

Skerrett, I.M., J.F. Smith, and B.J. Nicholson. 1999. Mechanistic differences between chemical and electrical gating of gap junctions. *In* Current Topics in Membranes. C. Peracchia, editor. Academic Press Inc., San Diego, CA. 249–269.

Skerrett, I.M., M. Merritt, L. Zhou, H. Zhu, F.-L. Cao, J.F. Smith, and B.J. Nicholson. 2000. Applying the *Xenopus* oocyte expression system to the analysis of gap junction proteins. *In* Methods in Molecular Biology. Connexin methods and protocols. R. Bruzzone and C. Giaume, editors. Humana Press, NJ. 225–249.

Sosinsky, G.E. 2000. Gap junctions structure: New structures and new insights. *In* Gap Junctions: The Molecular Basis of Cell Communication in Health and Disease. C. Peracchia, editor. Academic Press Inc., San Diego, CA. 1–22.

Spray, D.C., T. Kojima, E. Scemes, O. Suadicani, Y. Gao, S. Zhao, and A. Fort. 2000. "Negative" physiology: What connexin-deficient mice reveal about the functional role of individual gap junction proteins. *In* Gap Junctions – The Molecular Basis of Cell Communication in Health and Disease. Vol 49. C. Peracchia, editor. Academic Press Inc., San Diego, CA. 1–22.

Steinberg, T.H., R. Civitelli, S.T. Geist, A.J. Robertson, E. Hick, R.D. Veenstra, H.-Z. Wang, P.M. Warlow, E.M. Westphale, J.G. Laing, and E. Beyer. 1994. Connexin43 and connexin45 form gap junctions with different molecular permeabilities in osteoblastic cells. *EMBO J.* 13:744–750.

Suchyna, T.M., L.X. Xu, F. Gao, C.R. Fourtner, and B.J. Nicholson. 1993. Identification of a proline residue as a transduction element involved in voltage gating of gap junctions. *Nature.* 365:847–849.

Suchyna, T.M., J.M. Nitsche, M. Chilton, A.L. Harris, R. Veenstra, and B.J. Nicholson. 1999. Different ionic selectivities for connexins 26 and 32 produce rectifying gap junction channels. *Biophys. J.* 77:2968–2987.

Trexler E.B., F.F. Bukauskas, J. Kronengold, T.A. Bargiello, and V.K. Verselis. 2000. The first extracellular loop domain is a major determinant of charge selectivity in connexin46 channels. *Biophys. J.* 79:3036–3051.

Unger, M.V., N.M. Kumar, N.B. Gilula, and M. Yeager. 1999. Three-dimensional structure of a recombinant gap junction membrane channel. *Science*. 283: 1176–1180.

Veenstra, R.D. 1996. Size and selectivity of gap junction channels formed from different connexins. *J. Bioenerg. and Biomembr*. 28:327–337.

White, T.W. 2002. Unique and redundant connexin contributions to lens development. *Science.* 295:319–320.

Williams, D.B., and M.H. Akabas. 1999. γ-Aminobutyric acid increases the water accessibility of M3 membrane-spanning segment residues in γ-aminobutyric acid type A receptors. *Biophys. J.* 77:2563–2574.

Yeager, M., and B.J. Nicholson. 1996. Structure of gap junction intercellular channels. *Curr. Opin. Struct. Biol.* 6:183–192.

Zhou, X.W., A. Pfahnl, R. Werner, A. Hudder, A. Llanes, A. Luebke, and G. Dahl. 1997. Identification of a pore-lining segment in gap junction hemichannels. *Biophys J.* 72:1946–1953.